A Two-Stage Reduction Process for Silicon Production

Mitsuhiro Tada, and Masahiro Hirasawa

Institute for Advanced Materials Processing, Tohoku University,
2-1-1 Katahira, Aobaku, Sendai, 980-8511, Japan

(Received December 28, 1998; final form January 11, 1999)

ABSTRACT

A new "Two-Stage Reduction Process" is proposed for the production of high purity silicon. The porous SiC separates molten SiO_2 from an evacuated chamber. In the first stage, the molten SiO_2 reacts with SiC to produce gaseous SiO. In the second stage, SiO is sucked through the porous SiC wall and is reduced to Si. The fundamental potential of this process is examined by experiments and theoretical considerations. The conditions for the formation of Si are investigated. The Si formation rate and the rate controlling steps of this process are discussed on the basis of the kinetic theory.

1. INTRODUCTION

Mass production of silicon of higher purity than the conventional "metallurgical grade silicon" (MG-Si) /1-6/ is one of the key industrial factors which must be realized to attain low cost of production of the silicon solar cell. Considerable research works have been done aiming to achieve more effective refining of MG-Si /7,8/. However, no proposal has been made concerning the smelting process which is more flexible in the raw materials of SiO_2 and which gives higher purity outputs than the conventional electric arc furnace process. A strong demand for the investigation of novel smelting process exists in this context.

In the present study, the authors propose a "Two-stage Reduction Process" of SiO_2 as a potential novel process of silicon smelting. The concept of the process and the results of the preliminary experiments are given in the following sections.

2. CONCEPT OF THE NOVEL PROCESS

The basic idea of the "Two-Stage Reduction" process is illustrated in Figure 1. The porous SiC, permeable to gas constituents but impermeable to the liquid SiO_2, separates the molten SiO_2 bath and the outer space which is evacuated to a reduced pressure. Reactions in this process are composed of two stages. In the first stage, the molten SiO_2 reacts with porous SiC to produce gaseous SiO at the interface between SiO_2 and SiC [1st reduction stage]. Then SiO is sucked through the porous SiC filter and reduced to liquid Si in the outer space [2nd reduction stage].

By separating the two reduction steps from each other, it is expected that the transfer of impurity from

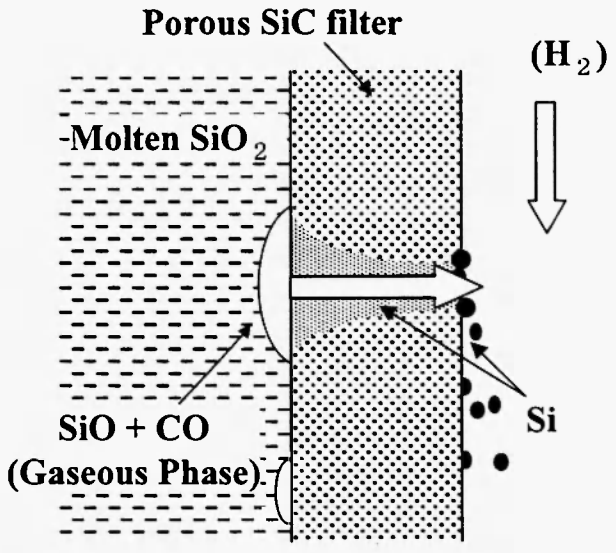

Fig. 1: The concept of two-stage reduction process of molten SiO_2

the raw material SiO_2 to the product Si is controlled under appropriately chosen conditions. The "Two-Stage Reduction Process" can be operated with more flexibility than the conventional electric arc furnace process. The aim of the present study is to prove the possibilities of the process and to investigate the fundamental mechanisms involved in the reactions.

3. EXPERIMENTAL

3.1 Experimental procedure

The experimental apparatus is shown schematically in Figure 2. The experimental temperature varies from T=2073 to 2273K. The furnace is a 15kW high frequency induction furnace. Quartz of 99.999pct purity is used as the charge. A porous SiC tube (13 mm in o.d., 7 mm in i.d. and 35 mm in length) with a closed bottom is connected to the vacuum system through a supporting tube which is made of graphite or SiC. A semiconductor pressure gauge is attached to the vacuum system for the measurement of the pressure inside the vacuum system.

A weighed amount (120g) of quartz is melted in a graphite crucible (50 mm in o.d. and 40 mm in i.d.) under Ar atmosphere. The depth of molten SiO_2 is 40mm. The temperature is measured by a thermocouple (W-5mass%Re/W-26mass%Re) at the top and bottom of the crucible. After the experimental temperature is established, the porous SiC tube is immersed in the molten SiO_2. The immersion depth of SiC tube is 35mm. Then the space inside the tube is evacuated and the experiment starts at this moment. The pressure inside the tube is 6.67×10^{4}Pa, which is attained within 1 min and is almost constant in most experiments. In a series of experimental runs, the inside space of the SiC tube is flushed with hydrogen gas at 0 to 50×10^{-6}Nm^3/min through a molybdenum nozzle.

At the end of the experiment, the evacuation is stopped and the SiC tube is pulled out from the SiO_2 bath. The SiC tube is then cooled down. The reaction product formed in the SiC tube is weighed. A part of the product is analyzed by the electron microprobe analyzer (EPMA) for bulk composition. The carbon content of the product is also measured by the combustion-IR absorption method with a LECO analyzer.

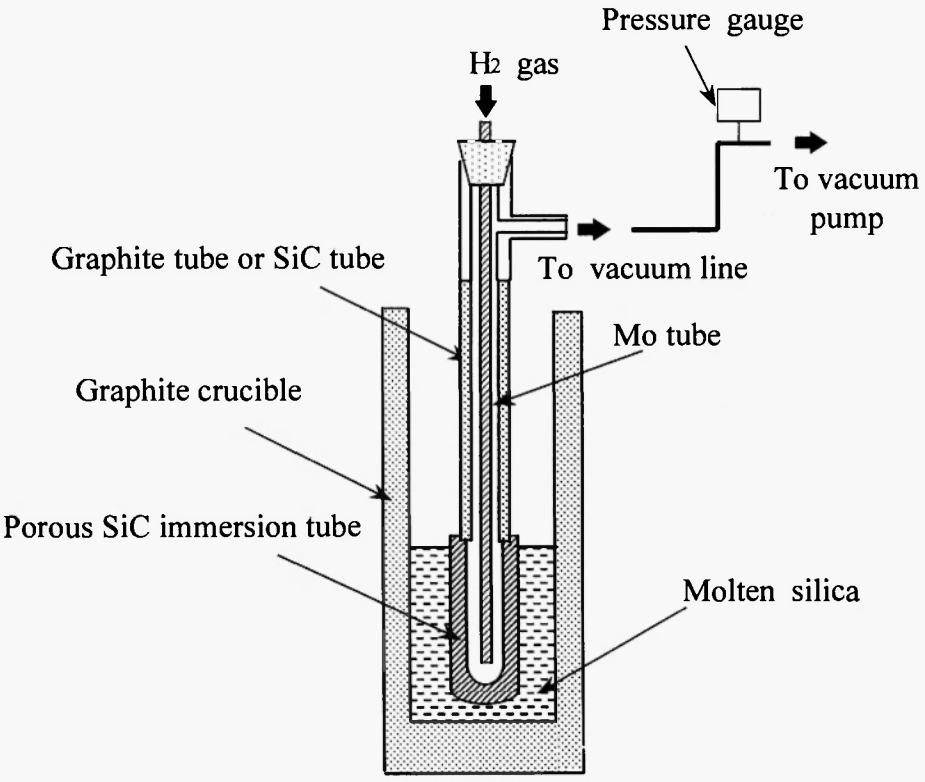

Fig. 2: Experimental apparatus

3.2 Preparation of porous SiC tube

We use a commercial reagent grade β-SiC powder (98% in purity) to produce the SiC tube. The average particle size of the SiC powder is 0.27μm. The powder is formed in the shape of a Tammann tube with a cold isostatic press machine (pressure: 200MPa), and the outer surface of the tube is shaped mechanically. The green body of the SiC tube is thus obtained, and the green body is sintered at ~2073K under argon atmosphere. The average micro pore size of the SiC tube is about 5 μm.

4. RESULTS AND DISCUSSION

4.1 Thermodynamic conditions for Si formation

Here, we examine the thermodynamic conditions of Si(l) existence in relation to the oxygen partial pressure, P_{O2}, and temperature for the Si-SiO-SiO_2-SiC system.

We consider the following reactions.

$$SiO_2(s) = SiO_2(l) \quad (1)$$
$$SiO_2(l) = SiO(g) + 1/2O_2(g) \quad (2)$$
$$SiO(g) = Si(l) + 1/2O_2(g) \quad (3)$$
$$SiO_2(l) = Si(l) + O_2(g) \quad (4)$$
$$Si(l) + CO(g) = SiC(s) + 1/2O_2(g) \quad (5)$$
$$2SiO_2(s \text{ or } l) + SiC(s) = 3SiO(g) + CO(g) \quad (6)$$

The relation between P_{O2} and temperature for the reaction equilibria of eqs.(2)~(6) are calculated under the following conditions

$$a_{SiO2} = 1 \text{ (for both l and s)} \quad (7)$$
$$a_{SiC} = 1 \quad (8)$$
$$P_{CO} / P^0 = 0.25 \quad (9)$$
$$P_{SiO} / P^0 = 0.75 \quad (10)$$
$$P_t = P_{CO} + P_{SiO} + P_{O2} + P_{CO2} = P^0 = 1.01325\times10^5 \text{ Pa} \quad (11)$$

Here, a_i is the activity of the component i; P_i is the partial pressure of component i; P_t is the total pressure ; P^0 is the standard pressure. It is to be noted that, considering the reaction of SiO(g) formation in the present reaction system of SiO_2 + SiC, the reaction which is described by eq.(6), we have taken the conditions of eqs.(9)~(11) for the gas phase components. In the calculation, we use the thermodynamic data in the literature /9/.

The results of the calculation are shown in Figure 3. In the figure, the solid lines represent the $G^\circ - T$ relation for the reactions of eqs.(2)~(6) at the equilibrium state. From the figure, we suppose that SiO(g) cannot be stable, while Si(l) can be stable, at $T >$ 2070K and $\log(P_{O2} / P^0) = -13.6$ under the condition of $a_{SiC} = 1$. It is to be noted that, from the thermodynamic viewpoint, the condition of Si(l) coexistence with SiC(s) is not affected by the location of the reduction, i.e. the gas-solid interface at the outer surface, the inner surface, or the wall micro pores of the SiC tube. This fact suggests that the possibilities of the two-stage reduction must be investigated with kinetic experiments, since the separation of Si(l) from SiO_2(l) is one of the key engineering factors of the process and the outer surface of the tube is not preferable as the site of Si(l) formation.

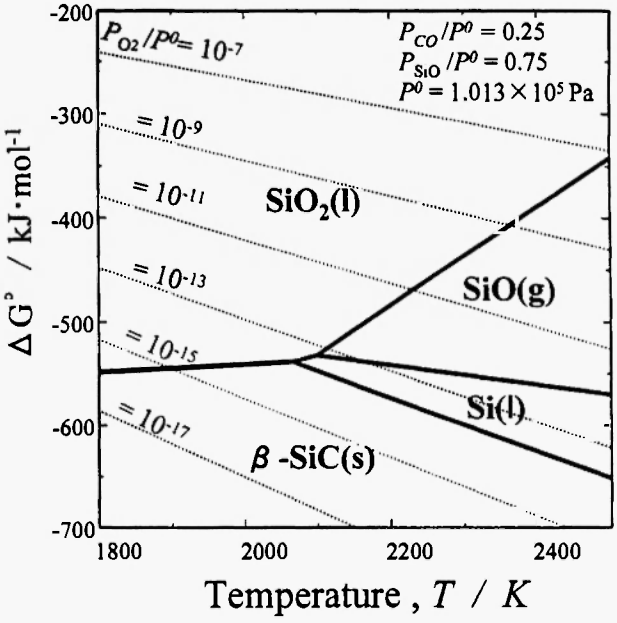

Fig. 3: The fields of phase stability in the system Si-O-C with $P_{CO}/P^0 = 0.25$ and $P_{SiO}/P^0 = 0.75$

4.2 Reduction of SiO_2(l) into SiO(g): 1st stage reaction

It has been well established that the reaction between SiO_2(l) and SiC(s) forms gaseous SiO(g) and

CO(g) as the products /10/. The kinetic details of the reaction have been not fully investigated.

In the present study, we have made preliminary experiments to confirm the formation of SiO(g) at the interface between molten SiO_2 and solid SiC tube. The experiments have been made at T = 2073K, at which the conversion from SiO to Si can be avoided (cf. Fig. 3). The experimental setup and the procedure are similar to those described in the section 3.1. After the experiments, we observed the inside and outside appearance of the SiC tube and the graphite supporting tube, and we found a small amount of brown material sticking inside the graphite supporting tube at the point of 50~200mm above the SiC tube's upper end. We qualitatively analyzed the brown material by usual chemical method and found that the material was an oxide of Si. At the same time, the results of the gravimetric analysis indicated that the composition of the oxide is SiO_{2-x} ($x \cong 0.4$). From these observations, we judge the brown material to be SiO partially oxidized by oxygen in the atmosphere. We consider that SiO(g), transferred from the SiO_2-SiC interface through the SiC tube wall, condensed inside the graphite supporting tube at the location where the wall temperature is considerably lower (~1473K) than 2073K. The amount of SiO_{2-x} is ~0.33g for an experimental run for 60min at T = 2073K. On the basis of the experimental results, we can conclude that the reduction of SiO_2(l) to SiO(g) and the suction of SiO(g) from the SiO_2-SiC interface are practically possible. The reality of the first stage of the two-stage reduction is thus confirmed.

4.3 Reduction of SiO(g) into Si(l): 2nd stage reaction

As indicated by Figure 3, we can expect that Si(l) can form at T > 2070K. Hence, to investigate second stage reaction, i.e. the reduction of SiO(g) into Si(l), we have made the experiments at T =2223K and T =2273K which are somewhat higher than 2070K.

Figure 4-a) shows the inside appearance of the SiC tube after an experiment at T = 2273K. The reaction time is 16 min from the start of the experiment. It is obvious that there exists a metal pool inside the SiC tube. It is to be noted that the color of the fracture of the SiC tube appears similar to that of the metal pool, and

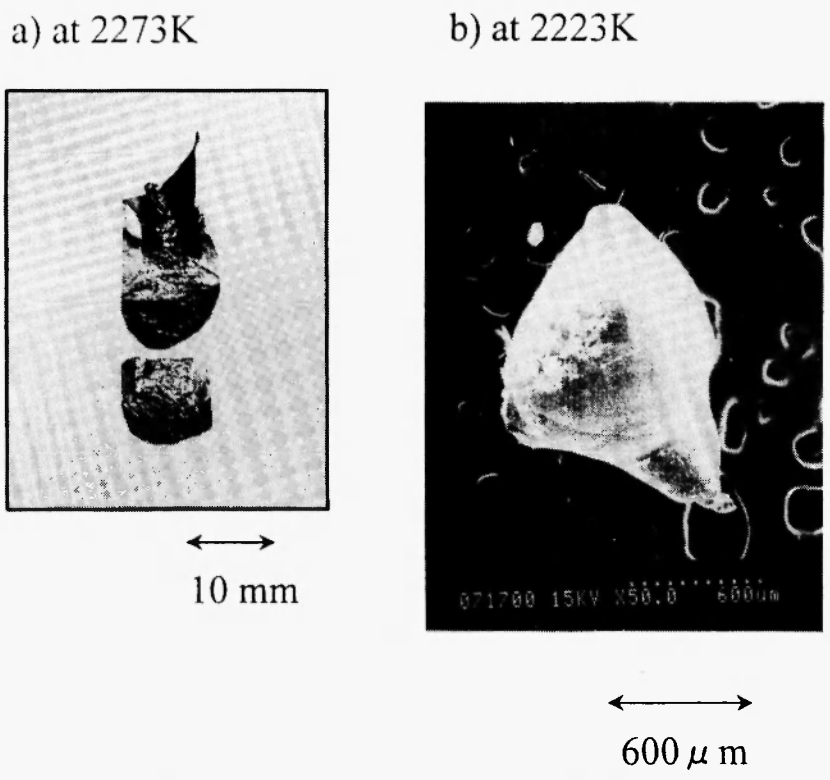

Fig. 4: Reaction products in the SiC tube

no green part, which indicates the existence of porous β-SiC, is obvious after the experiment. It is also to be noted that we cannot observe any trace of SiO inside the SiC tube and the graphite supporting tube in the experiments at $T > 2223$K.

We examine the atomic composition of the metallic product inside the SiC tube by characteristic X-ray analysis with a SEM-EDS (Scanning Electron Microscopy - Energy Dispersive X-ray Spectrometer) combined equipment. A typical result of the measurement of the spectrum of X-ray emitted from a small piece of the metal sample is illustrated in Figure 5, where the X-ray intensity (arbitrary unit) is plotted against the energy of X-ray. We observe, in Figure 5, a strong peak at 1.74keV, which corresponds to the K_α-ray of Si, with the continuous X-ray as a back ground. The K_α-ray of Si is the only one characteristic X-ray in the spectrum. From this fact, we can deduce that the metal in the SiC tube consists of Si.

In the experiments at T=2223K, on the other hand, we can also observe the formation of metal Si inside the SiC tube. However, the amount of Si is considerably smaller than that obtained at T=2273K, and the metal Si appears in the form of droplets, which is shown in Figure 4-b), instead of a metal pool.

The carbon content of Si obtained from the experiment at T = 2273K is analyzed and the results of the analysis are shown in Figure 6. In the figure the dotted line represents the solubility of carbon in liquid Si in equilibrium with SiC /11/ at T = 2273K. As seen in the figure, [mass%C] in Si ranges from 0.05 to 0.2. The carbon content is close to that of the carbon solubility, which is coincident with the fact that the Si melt is contained in the SiC tube.

From the fact that Si metal is observed inside the SiC tube in the experiments at T = 2223K and 2273K, we conclude that the second stage reaction, i.e. the

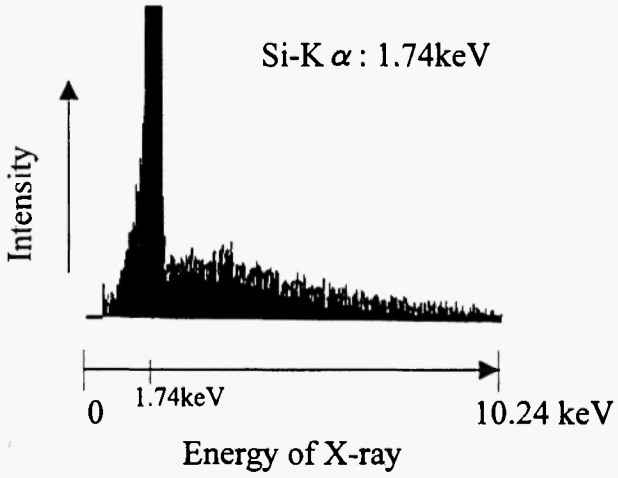

Fig. 5: The result of SEM-EDS measurement for the metal

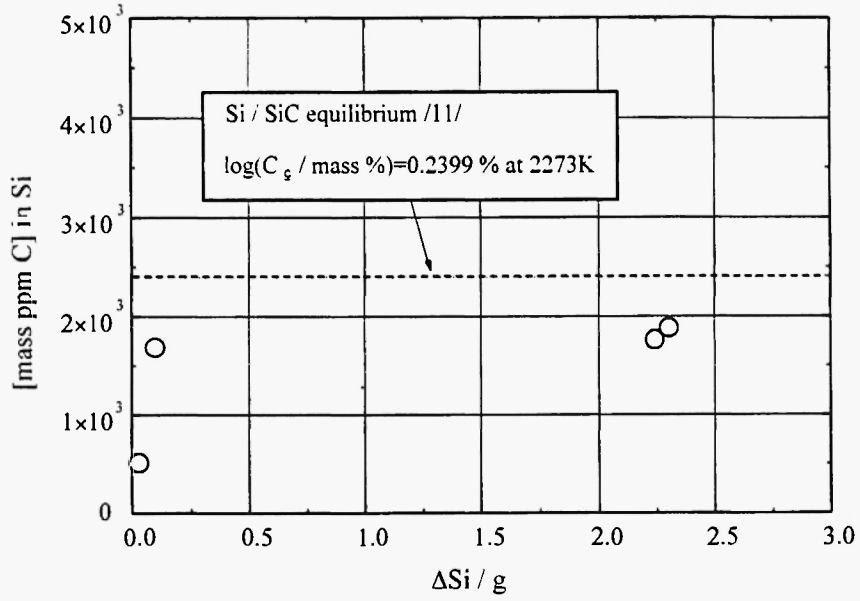

Fig. 6: Relation between mass of produced Si and [mass ppm C]

reduction of SiO into Si, takes place at $T > 2223$K in the transportation process through the porous SiC tube wall. We thus can confirm the positive possibilities of the two-stage reaction process for the reduction of SiO_2 into Si.

To confirm the reduction of SiO by SiC in more detail, we have examined the effect of additional reductant on the amount of Si. As the additional reductant, we have employed H_2 which was supplied inside the SiC tube through the molybdenum tube shown in Figure 2. The experiments have been made at T = 2273K for t = 16~17min. The results of the experiments are shown in Figure 7. As seen in the figure, the amount of Si, ΔSi, obtained from the experiments, is almost constant at ~2g under the present experimental condition, and no influence of the flow rate of H_2 is apparent. This fact indicates that no additional reductant is necessary for the 2nd stage reduction of SiO, and SiO formed in the 1st stage reduction is fully reduced to Si by SiC.

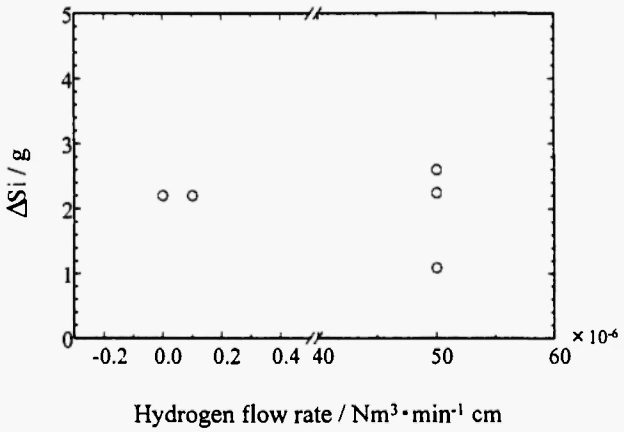

Fig. 7: Effect of hydrogen flow rate on the amount of Si formed by the reaction

4.4 Change in the gas composition in the reaction process

As described in 4.1, we found no trace of unreacted SiO in the SiC tube and the graphite supporting tube in the experiments at $T > 2223$K, and, in these cases, only the carbon supplied from SiC acts as the reductant.

The reaction between SiO_2(l) and SiC(s) is written as

$$2SiO_2\,(l) + SiC(s) = 3SiO(g) + CO(g) \qquad (12)$$

which is the overall reaction of the 1st stage reduction and takes place at the SiC-SiO_2 interface.

The reaction between SiO(g) and SiC(s) is represented by

$$SiO(g) + SiC(s) = 2Si(l) + CO(g) \qquad (13)$$

which is the overall reaction of the 2nd stage reduction and takes place at the gas-solid interface in the micro pores of the porous SiC tube wall.

According to the reactions of eq. (12) and (13), we have SiO and CO as the components of the gas phase. Hence we have to consider that the gas phase product of SiO+CO mixture is transported from the SiO_2-SiC interface to SiC tube's inside space, through the SiC tube wall, with changing its own composition. Here, we examine the change in P_{SiO} and P_{CO} in the reaction gas by thermodynamic phase relations. Here, it is to be noted that the coexistence of SiO_2 with SiC (and C) is impossible under the conditions of $T < 2273$K and $P_t / P^\circ = 1$ from a thermodynamic viewpoint /9/.

(1) Equilibrium gas composition at the reaction interface

Since SiO_2(l) cannot coexist with SiC(s) in the equilibrium state, a gas phase, i.e. bubble or gas film, must separate the two condensed phases. Assuming a gas film between SiO_2(l) and SiC(s), we have two interfaces. The composition of the gas-side of the two interfaces must be different and this difference in the gas composition originates the driving force of the 1st stage reduction. Here, we estimate the equilibrium composition of the gas phases at the SiO_2(l)-gas and SiC(s)-gas interfaces. Further kinetic analysis is to be made in a later section **4.5**.

(i) SiC(s)-gas interface

The reactions at this interface are represented by the following equations. Here, we assume the formation of Si(l) by the reduction of SiO(g).

$$SiO(g) + SiC(s) = 2Si(l) + CO(g) \quad (13)$$

$$K_{13} = \frac{a_{Si}^2 P_{CO}}{P_{SiO} a_{SiC}} = 1.086 \text{ [at } T = 2273\text{K]} \quad (14)$$

$$CO_2(g) = CO(g) + 1/2O_2(g) \quad (15)$$

$$K_{15} = \frac{P_{CO} P_{O_2}^{1/2}}{P_{CO_2}} = 1.105\times10^{-2} \text{ [at } T = 2273\text{K]} \quad (16)$$

$$CO_2(g) + SiC(s) = Si(l) + 2CO(g) \quad (17)$$

$$K_{17} = \frac{a_{Si}^2 P_{CO}}{P_{CO_2} a_{SiC}} = 1.85\times10^{4} \text{ [at } T = 2273\text{K]} \quad (18)$$

Here, the equilibrium constants are calculated with the thermodynamic data /9/. Then we have, at T = 2273K,

$$(P_{SiO})_{(i)}/P^0 = 0.479, \quad (19)$$
$$(P_{CO})_{(i)}/P^0 = 0.521, \quad (20)$$
$$(P_{CO2})_{(i)}/P^0 = 1.46\times10^{-5}, \quad (21)$$
$$(P_{O2})_{(i)}/P^0 = 9.66\times10^{-14}. \quad (22)$$

where $P_t = P_{CO} + P_{SiO} + P_{O2} + P_{CO2} = P^0$ and $a_{SiC} = a_{Si} = 1$.

It is to be noted that the SiC(s)-gas interface can locate in the wall of the porous SiC tube in the present study.

(ii) SiO_2(l)-gas interface

The following reaction together with the reaction of eq.(15) is considered for the equilibrium at the interface between SiO_2(l) and gas.

$$SiO_2(l) + CO(g) = SiO(g) + CO_2(g) \quad (23)$$

$$K_{23} = \frac{P_{SiO} P_{CO_2}}{a_{SiO_2} P_{CO}} = 7.507\times10^{-3} \text{ [at } T = 2273\text{K]} \quad (24)$$

Under the condition of $a_{SiO2} = 1$ and $P_t / P^0 = 1$, the changes in P_{SiO}, P_{CO}, P_{CO2} with P_{O2} at 2273K are calculated on the basis of eqs.(16) and (24). The results of the calculation are shown in Figure 8. The partial pressures of the SiC(s)-gas interface are also plotted in the figure.

From Figure 8, considering the non-zero driving forces for the transportation of SiO, CO and CO_2 in the gas phase, we have

$$0.479 < (P_{SiO})_{(ii)}/P^0 < 0.973 \quad (25)$$
$$2.68\times10^{-2} < (P_{CO})_{(ii)}/P^0 < 0.520 \quad (26)$$
$$1.46\times10^{-5} < (P_{CO2})_{(ii)}/P^0 < 5.78\times10^{-4} \quad (27)$$
$$3.66\times10^{-11} < (P_{O2})_{(ii)}/P^0 < 1.51\times10^{-10} \quad (28)$$

(2) Changes in P_{SiO} and P_{CO} with the proceeding of the reduction process

(iii) 1st stage reduction

The first stage reduction of SiO_2 takes place at the SiO_2(l)-SiC(s) interface, and a gas bubble or gas film is formed between SiO_2(l) phase and SiC(s) phase. The gas phase thus covers the surface of the SiC tube to some extent.

The gas composition at SiO_2-gas interface can be

$$P_{SiO}^{SiO_2/Gas} = (P_{SiO})_{(ii)} \quad (29)$$
$$P_{CO}^{SiO_2/Gas} = (P_{CO})_{(ii)} \quad (30)$$
$$P_{CO2}^{SiO_2/Gas} = (P_{CO2})_{(ii)} \quad (31)$$

Here, the superscript SiO_2/Gas indicates the SiO_2-gas interface. The actual numerical values for $P_{SiO}^{SiO_2/Gas}$ etc. are not determined only by the thermodynamic relations but also by the kinetic relations which restrict the fluxes of SiO etc. in the gas phase.

At the SiC tube surface covered by the bubble (or gas film), the composition of the gas phase, i.e. $P_{SiO}^{SiO_2/Gas}$ and $P_{CO}^{SiO_2/Gas}$, should be

$$P_{SiO}^{SiO_2/Gas}/P^0 > P_{SiO}^{SiC/Gas}/P^0 > 0.479 \quad (32)$$

$$P_{CO}^{SiO_2/Gas}/P^0 < P_{CO}^{SiC/Gas}/P^0 < 0.521 \quad (33)$$

The difference in the composition at the two interfaces causes mass transport of SiO and CO(and also CO_2) in the bubble (or gas film).

(iv) 2nd stage reduction

Because of the pressure gradient between the

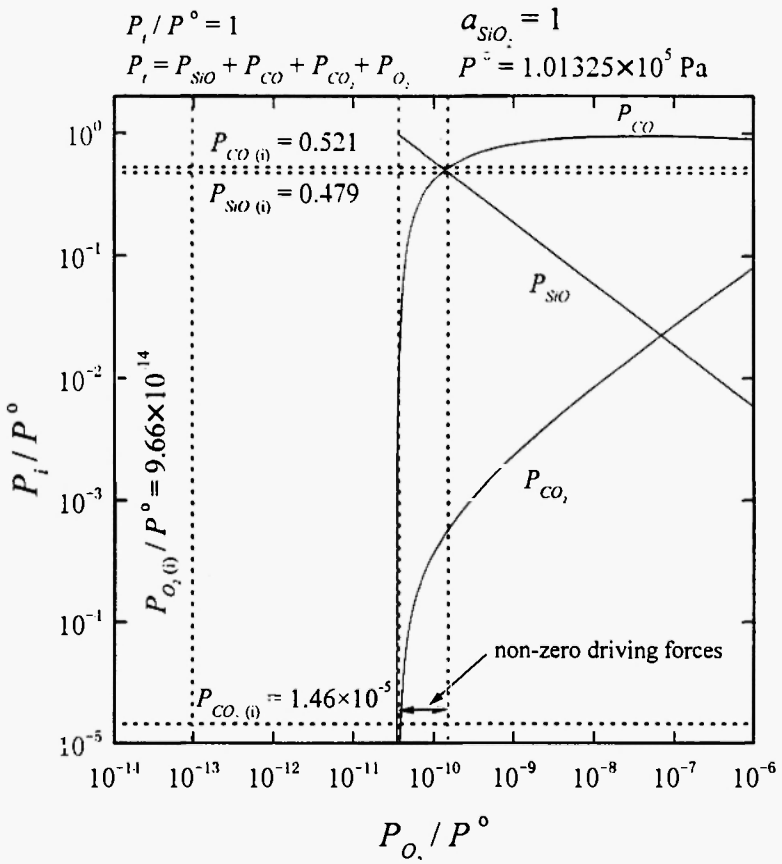

Fig. 8: Relation between P_{O2} and P_{CO}, P_{SiO} and P_{CO2} at $T = 2273$K and $P^0 = 1.01325\times10^5$ Pa

SiO_2-SiC interface (~normal pressure) and the inside space of the SiC tube ($1.01325\times10^5 > P > \sim6.67\times10^4$ Pa), the gas mixture of SiO+CO(+CO_2+O_2) is transferred from the SiO_2(l)-SiC(s) interface to the pores in the SiC tube wall. Here, we assume that the 2nd stage reduction of SiO into Si takes place in the wall pores but we do not need to fix the location of the pore, where the Si formation is taking place, for the purpose of the present discussion.

At the SiC-gas interface of the micropore in the SiC tube wall, the reduction of SiO by SiC takes place and Si(l) forms at the interface. The gas composition of the gas side interface is then represented by

$$P_{SiO,i}^{Pore} / P^0 = 0.479 \tag{34}$$

$$P_{CO,i}^{Pore} / P^0 = 0.521 \tag{35}$$

under the condition of $P_t = P^0$, or by

$$P_{SiO,i}^{Pore} / P^0 = 0.315 \tag{36}$$

$$P_{CO,i}^{Pore} / P^0 = 0.342 \tag{37}$$

under the condition of $P_t = \sim6.67\times10^4$ Pa.

It is to be noted that the partial pressures of SiO and CO, P_{SiO} and P_{CO}, in the bulk gas inside the micropore must be

$$P_{SiO}^{SiC/Gas} / P^0 > P_{SiO} / P^0 > P_{SiO,i}^{Pore} / P^0 \tag{38}$$

$$P_{CO}^{SiC/Gas} / P^0 < P_{CO} / P^0 < P_{CO,i}^{Pore} / P^0 \tag{39}$$

When the gas mixture consisting of SiO and CO with a small amount of CO_2 and O_2 transfers from the SiC tube's outer surface to the inside space of the tube, P_{SiO} decreases and P_{CO} increases simultaneously, with the proceeding of Si(l) deposition at the SiC-gas interface in the micropores in the SiC tube wall. The deposition of Si(l) terminates at a point where the bulk partial pressures of SiO and CO attain to $P_{SiO,i}^{Pore}$ and $P_{CO,i}^{Pore}$, respectively.

(3) Gas-metal reactions

According to the thermodynamic estimation of the reaction gas composition, we have to expect that, after the reduction of SiO(g) into Si(l) terminates, there still remains a considerable amount of SiO in the reaction gas because the lower limit for P_{SiO} is determined as $P_{SiO,i}^{Po\text{-}e}$ from the equilibrium conditions.

If the remaining amount of SiO is removed from the reaction system without further reaction, we must observe the deposition of SiO in the graphite supporting tube (c.f. 4.2) at a low temperature zone. In the experiments at T = 2223K and 2273K, however, we found no trace of SiO deposition (c.f. 4.2). This fact suggests that SiO is consumed by some other reaction than eq. (13), and that the overall reaction does not reach to the equilibrium state.

The possible reaction, which can decrease SiO to the lower level than the equilibrium estimation of $P_{SiO,i}^{Po\text{-}e}$, is represented as follows

$$SiO + \underline{C} \text{ (in Si(l))} = Si(l) + CO(g) \qquad (40)$$

since Si(l) contains a considerable amount of C (c.f. 4.3).

Considering the fact that we pump out CO continuously during the experiments, we can expect the proceeding of the reaction of eq. (40) on the basis of LeChatelier's principle. If the reaction of eq.(40) takes place, we can also expect that C concentration in the liquid Si becomes lower than that under the equilibrium condition of Si(l)-SiC(s) system. This expectation is consistent with the results shown in Figure 6, where [mass ppm C] is slightly lower than that at the equilibrium at T = 2273K. We thus conclude that P_{SiO} in the gas phase is negligible above the molten Si bath in the SiC tube owing to the gas-metal reaction represented by eq. (40). In this context, we need not consider the reoxidation of SiO by CO although P_{CO} increases with the decrease in P_{SiO}. The details of the gas-metal reaction, e.g. the interfacial area, the shape of the interface (bubble or not) etc., are to be investigated in a future study.

4.5 Reaction kinetics of the two-stage reduction process

As has been described in 4.3, the amount of Si, which results from the 2nd reduction process, is very much smaller at T = 2273K. On the basis of this fact, we discuss the kinetic aspects of the present reduction process qualitatively in the following.

4.5.1 Apparent Si formation rate

The amount of Si, ΔSi, obtained from the experiments under various reaction conditions is shown in Figure 9 in which the data represented by ● are those obtained from the experiments at T < 2273K for the reaction time, t, of t = 60min. The data represented by ○, ▲, △, ■ and □ are those obtained from the experiments at T = 2273K for t = 10~17min. It is to be noted that ΔSi / mg = 0 at T = 2073K.

The observations deduced from Figure 9 are summarized as

(i) obvious dependence of ΔSi on T, and

(ii) large ΔSi for a longer reaction time at T = 2273K.

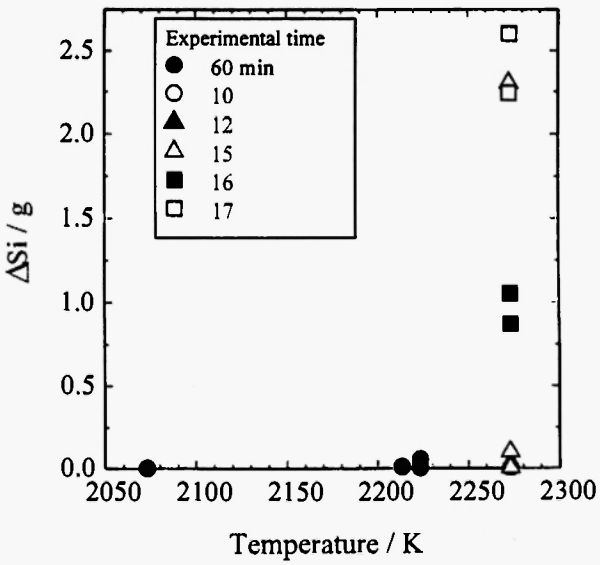

Fig. 9: Relation between produced Si and temperature

4.5.1.1 Relation between ΔSi and time at T = 2273K

Here, we examine the change in ΔSi with the reaction time, t, for the data obtained from the experiments at T = 2273K. Figure 10 shows the relation between ΔSi and t. In the figure, ○ represents the data shown in Figure 9.

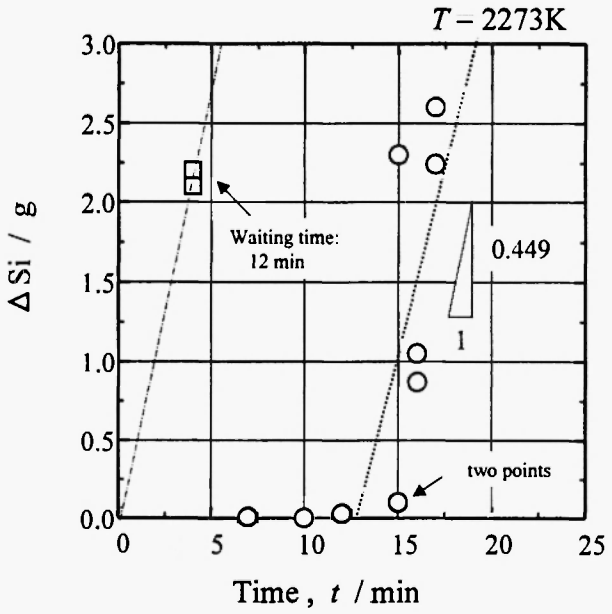

Fig. 10: Relation between the reaction time and the mass of Si(l) obtained from the experiments

Apparently, ΔSi increases with increasing the reaction time at t > ~12min, while, at t < ~12min, ΔSi is very small compared with that at t > ~12min. Here, we should note that, in the experiments which give the data of ○ in the figure, the reaction time has been measured from the time point at which the porous SiC tube has been immersed in the molten SiO_2. In this case, we have to consider that the temperature of the porous SiC tube is considerably lower than that of the molten SiO_2 bath at the instance of the immersion, owing to the large temperature gradient in the space above the graphite crucible which is heated inductively. The immersion of the SiC tube hence lowers the temperature of the molten SiO_2 bath. The overall reaction of Si formation is retarded thereby (c.f. Figure 9 where ΔSi is small at T < 2223K) for the initial 12min until the bath temperature and also the temperature of the SiC tube reach again their initial condition of T = ~2273K. We thus can explain the small ΔSi at t < ~12 min in Figure 10 by considering the cooling effect. To examine the cooling effect in more detail, we have made several experiments in which the suction of SiO (+CO) gas into the inside space of the SiC tube has been started after 12 min from the immersion of the tube (waiting time). The reaction time in these cases is 4 min. The results of the experiments are illustrated by □ in Figure 10. As seen in the figure, ΔSi in these trials with the waiting time are ~2.2g which is comparable to ΔSi = 2.2~2.5g obtained in the experiments without the waiting time for t = ~16 min. This fact clearly indicates the cooling effect. Here, it is to be noted that, in preliminary experiments without suction for more than 30 min, we have observed the apparent absence of Si formation at the SiC-SiO_2 interface even at T = 2273K. This observation justifies the performance of the experiments with the waiting time.

4.5.1.2 Evaluation of Si formation rate

From the experimental results shown in Figure 10, we evaluate the apparent Si formation rate, $\frac{d\Delta Si}{dt}$, by linear fitting of the data of t > ~12 min. The result of the least square fitting is indicated by the dotted line in Figure 10. From the slope of the linear line, we have

$$\frac{d(\Delta Si / g)}{d(t / min)} = 0.449$$

at T = 2273K.

With the data represented by □ in Figure 10, we take $\Delta Si/\Delta t$, where Δt is the reaction time, as the apparent Si formation rate at the same temperature of T = 2273K, since, in these experiments, the temperature is considered as constant throughout the reaction time.

For T = 2223K, we also evaluate the apparent Si formation rate by taking $\Delta Si/\Delta t$, because, at T = 2223K, the reaction time is 60min which is considered as long enough to assure the establishment of the steady state for the heating condition.

The apparent Si formation rates obtained from the experimental results are plotted against the experimental temperature in Figure 11. The figure shows that the apparent rate of Si formation increases from ~0.1 mg/min at T = ~2223K to ~100 mg/min at T = 2273K with increasing temperature.

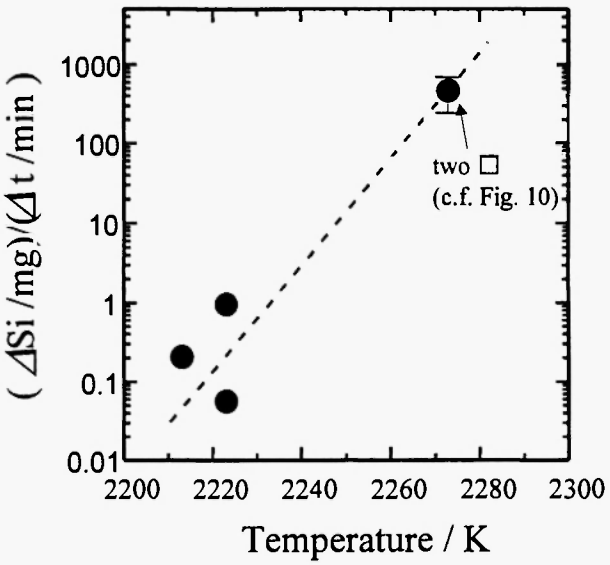

Fig. 11: Relationship between temperature and Si/ t

4.5.2 Evaluation of SiO formation rate

As described in 4.1, we observed no accumulation of SiO in the SiC tube (and the graphite supporting tube) in the experiments at T = 2223K and T = 2273K. From this observation, we conclude that whole amount of SiO formed in the 1st reaction stage is reduced rapidly to Si in the 2nd reaction stage, and the 2nd reaction stage does not control the overall reaction rate of the present process. Thus we have to consider that the rate controlling step is involved in the 1st stage reaction. To confirm this consideration, we need to estimate the rate of SiO formation from our experimental results.

The rate of SiO formation, $\Delta SiO/\Delta t$, in the 1st stage reaction is evaluated by the experimental results as follows.

For the experiments at T = ~2223K and T = 2273K, $\frac{d\Delta SiO}{dt}$ is evaluated with the following relation on the assumption that $\Delta SiO = \Delta Si \times 1/2$ according to the reaction of eq. (13).

$$\frac{d\Delta SiO}{dt} = \frac{d\Delta Si}{dt} \times \frac{1}{2} \quad \text{or} \quad \frac{\Delta Si}{\Delta t} \times \frac{1}{2}$$

where $\frac{d\Delta Si}{dt}$ and $\frac{\Delta Si}{\Delta t}$ represent the apparent Si formation rate estimated in 4.5.1.2.

For the experiments at T = 2073K, we evaluate the apparent rate with simply dividing the amount of SiO_{2-x}, obtained as the deposit inside the graphite supporting tube, by the experimental time.

The relation between the apparent SiO formation rate and temperature is illustrated in Figure 12. Obviously the apparent SiO formation rate is less than 0.01g/min and does not change in the temperature range of T – 2073~2223K. On the other hand, between T = 2223K and T = 2273K, $\frac{d\Delta SiO}{dt}$ increases with the increase in temperature. The strong dependence of the apparent SiO formation rate on the temperature in the narrow range of T = 2223~2273K shows strikingly high contrast to the independence of the apparent SiO formation rate on the temperature in the much wider range of T = 2073~2223K.

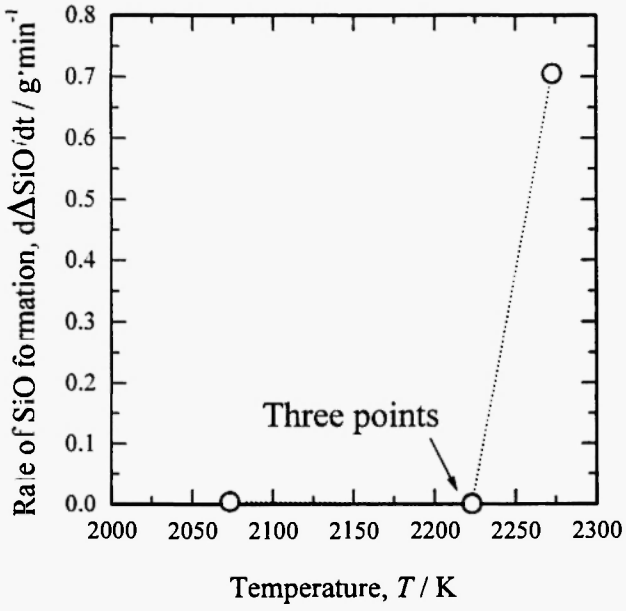

Fig. 12: Relationship between d SiO/dt and temperature.

4.5.3 Elementary steps of the reaction of the 1st stage

From the general theory of reaction kinetics, we can divide the overall reaction of the 1st stage reduction of SiO_2 into SiO in several elementary reaction steps as follows.

(i) Chemical reaction at SiO_2(l)-SiC(s) interface:

$$2SiO_2(l) + SiC(s) = 3SiO(g) + CO(g) \quad (12)$$

(ii) Chemical reaction at gas- $SiO_2(l)$ interface:

$$SiO_2(l) + CO(g) = SiO(g) + CO_2(g) \quad (23)$$

(iii) Mass transfer of CO and CO_2 in the gas phase (bubble or gas film) between the gas- $SiO_2(l)$ interface and the gas-SiC(s) interface:

Step (a) is the direct reaction in which the reductant, SiC, is supplied directly to the reaction interface. Step (b), on the other hand, is the indirect reaction between SiO_2 and SiC. Step (b) is combined with Step (c) in which the oxygen atom concerning the reduction is carried by CO and CO_2 (ferrying effect).

As for the rate controlling step of the present reaction, however, the three steps cannot correspond to it, since none of the kinetic factors of the three steps, e.g. chemical rate constants, diffusion coefficients etc., can change irregularly with temperature like $\frac{dn_{SiO}}{dt}$ in Figure 12. Arrheniusian behaviors are the usual forms of the relations between the kinetic parameters and temperature. The relations between the kinetic parameters and temperature can be interpreted theoretically as follows.

Here, we consider the following rate equations representing the SiO formation rate.

$$\frac{dn_{CO}^{L/G}}{dt} = A_{L/G}\frac{k_{CO}}{RT}\left(P_{CO} - P_{CO}^{L/G}\right) \quad (41)$$

$$\frac{dn_{CO_2}^{L/G}}{dt} = A_{L/G}\frac{k_{CO2}}{RT}\left(P_{CO_2}^{L/G} - P_{CO_2}\right) \quad (42)$$

$$\frac{dn_{SiO}^{L/G}}{dt} = A_{L/G}\left(k_R P_{CO}^{L/G} - k_{OX} P_{SiO}^{L/G} P_{CO2}^{L/G}\right) \quad (43)$$
$$= A_{L/G} k_{SiO}\left(P_{SiO}^{L/G} - P_{SiO}\right)$$

$$\frac{dn_{CO}^{L/G}}{dt} = \frac{dn_{CO2}^{L/G}}{dt} = \frac{dn_{SiO}^{L/G}}{dt} \quad (44)$$

$$\frac{dn_{SiO}^{L/S}}{dt} = A_{L/S} k'_{L/S} \quad (45)$$

$$\frac{dn_{SiO}^{OV}}{dt} = \frac{dn_{SiO}^{L/G}}{dt} + \frac{dn_{SiO}^{L/S}}{dt} \quad (46)$$

where: n_i is the mol of i-component; P_i is the partial pressure of i-component; C_i is the mol concentration of i-component; k_{CO} and k_{CO2} are the mass transfer coefficients of CO and CO_2, respectively, in the gas phase (a bubble or gas film); k_R and k_{OX} are the rate constants of the reaction of eq. (23) for the forward and the backward directions, respectively; k' is the rate constant for the forward reaction of eq. (12), respectively; $A_{L/G}$ and $A_{L/S}$ are the interfacial areas between the liquid SiO_2 and the gas phases and between the liquid SiO_2 and the solid SiC phases, respectively; and superscript ov represents overall rate. The superscript L/G and L/S represent the liquid-gas and liquid-solid interfaces, respectively.

The equation (46) represents the overall rate of SiO formation, and the equations (43) and (44) are the conditions of the steady state for the reactions at gas-liquid interface. Considering the unit activity of SiO_2 and SiC, we assume apparent 0th order reaction rate (= constant rate) in eq. (45). The apparent rate constant, $k'_{L/S}$, can be affected by the porosity of the SiC tube.

From eqs. (41) ~ (46), we have the following equation for the overall rate of SiO formation.

$$\frac{dn_{SiO}^{OV}}{dt} = A_{L/G} k_{OV}^{L/G}\left(P_{SiO,e} - P_{SiO}\right) + A_{L/S} k'_{L/S} \quad (47)$$

$$\frac{1}{k_{OV}^{L/G}} = \frac{1}{KP_{CO2}}\left\{\left(\frac{RT}{k_{CO}} + \frac{1}{k_R}\right) + \frac{RT}{k_{CO2}} K P_{SiO}^{L/G}\right\} + \frac{1}{k_{SiO}} \quad (48)$$

$$P_{SiO,e} = K_{23}\frac{P_{CO}}{P_{CO2}} \quad (49)$$

$$K = \frac{k_{OX}}{k_R} \quad (50)$$

We can expect that the chemical rate constants k_R and $k'_{L/S}$ should increase with increasing temperature according to the Arrhenius's relation in the narrow temperature range of T = 2073~2273K

$$k_R = k_{R,0} \exp(-\frac{E_R}{RT}) \quad (51)$$

$$k'_{L/S} = k_{L/S,0} \exp(-\frac{E_{L/S}}{RT}) \quad (52)$$

where $k_{R,0}$ and $k'_{L/S,0}$ are the frequency factors and E_R and $E_{L/S}$ are the activation energies.

At the same time, we can also expect Arrheniusian relations for the diffusion coefficients of CO, SiO and CO_2. We hence expect that k_{CO}, k_{CO2} and k_{SiO} increase with temperature and thereby $k_{OV}^{L/G}$ increases monotonously with increasing temperature. The change in the dependence of SiO formation rate on the temperature in the present experiments (Fig. 12) cannot be caused by the changes in the kinetic constants, i.e. the chemical rate constants and the mass transfer coefficients.

In eq. (47), except for the kinetic constants, the interfacial areas, $A_{L/G}$ and $A_{L/S}$, are the factors which can affect the rate of SiO formation. We have to investigate if the interfacial areas change with the temperature.

4.5.4 Interfacial areas for SiO formation reaction – Observation of the surface of the SiC tube

To obtain the information concerning the interfacial areas of gas-liquid SiO_2, gas-solid SiC, and the liquid SiO_2-solid SiC interfaces in the vicinity of the outer surface of the SiC tube, we observe the surface of the SiC tube after the experiments.

The outer surfaces of SiC tubes used in the experiments at T = 2073K and 2273K are shown in Figure 13.

It is seen in the figure that the traces of the reaction, i.e. the decrease in the tube's diameter, small pit holes etc., are evident in both cases. But there is a considerable difference in the wetting behavior of SiO_2 between T = 2073K and 2273K. In the case of T = 2073K, we observe no trace of wetting by SiO_2. We can hardly imagine that the SiC tube's surface contacted directly with the liquid SiO_2 in this experiment. In the case of the SiC tube used in the experiment at T – 2273K, a comparatively large part of the SiC surface is wet by SiO_2. The direct contact of SiC with liquid SiO_2 is evident in this case.

On the basis of the above mentioned observation, we imagine that, at the lower temperature of T = 2073K and 2223K, there is almost no direct contact of the solid SiC tube surface with the liquid SiO_2 during the experiment, while, at T = 2273K, the direct reaction (eq. (12)) at the liquid SiO_2-solid SiC interface takes part in the formation of SiO.

The difference in the SiO_2-SiC contact between T = 2073~2223K and T = 2273K is also supported by the following observations. At the end of the experiments, the SiC tube was withdrawn from the SiO_2 bath. In the experiments at T = 2073~2223K, the fluidity of the liquid SiO_2 was very small and a hole with a similar diameter to that of the SiC tube was left in the SiO_2 bath after the SiC tube was withdrawn. In the experiments at T = 2273K, no hole was observed and a small amount of very viscous SiO_2 stringing and adhering to the SiC tube surface came out with the SiC tube.

The formation of the hole in the SiO_2 bath after the experiments at T = 2073~2223K is interpreted as follows.

At the initial contact of the SiC tube with the SiO_2 bath, gaseous reaction products, i.e. SiO and CO, form at the SiC-SiO_2 interface. This gas phase forms a thin gas film between the SiC tube and SiO_2 bath. At T – 2073~2223K, the fluidity of the liquid SiO_2 is very low because of the very high viscosity. The liquid flow in the SiO_2 bath does not grow so as to break the thin gas film although the suction of the gas through the tube's wall enhances the contact of SiC with molten SiO_2.

The viscosity coefficient /12/ of molten SiO_2 is shown in Figure 14. As seen in the figure the viscosity coefficient, μ, is as high as 10^4 ~10^5 Pa s at T = 2073~2273K. With this high viscosity, the Reynolds number for the liquid flow in the SiO_2 bath becomes very small (~10^{-5}) for the usual flow velocity (several cm/s) related to the characteristic ascending motion of a bubble of ~10mm in diameter. In this case, intensive flow cannot grow, which verifies the interpretation of the hole formation stated above.

At T = 2273K, μ =~5×10^4 Pa s which is still very high but is comparatively lower than the value at T =

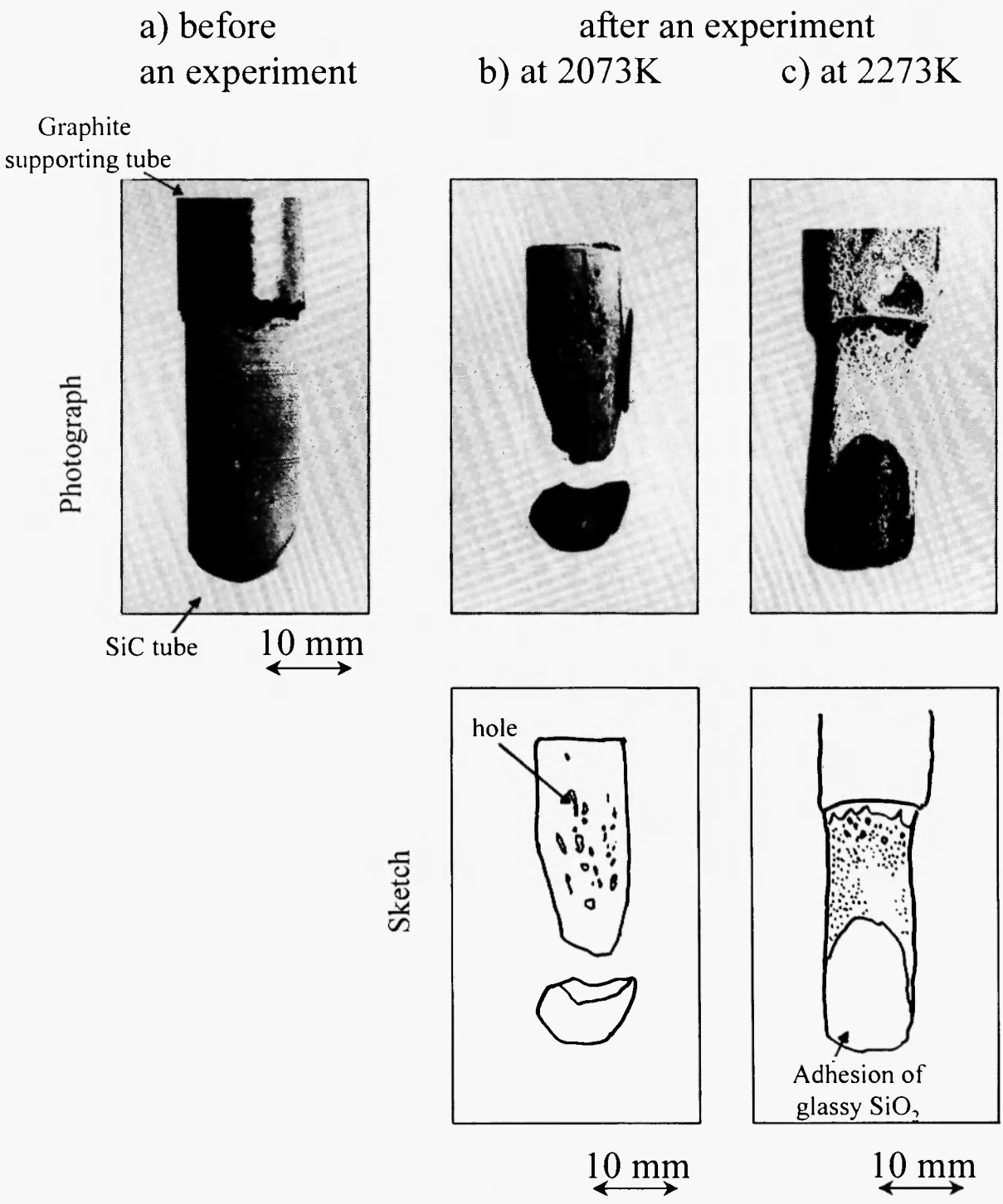

Fig. 13: Surface of SiC tube.

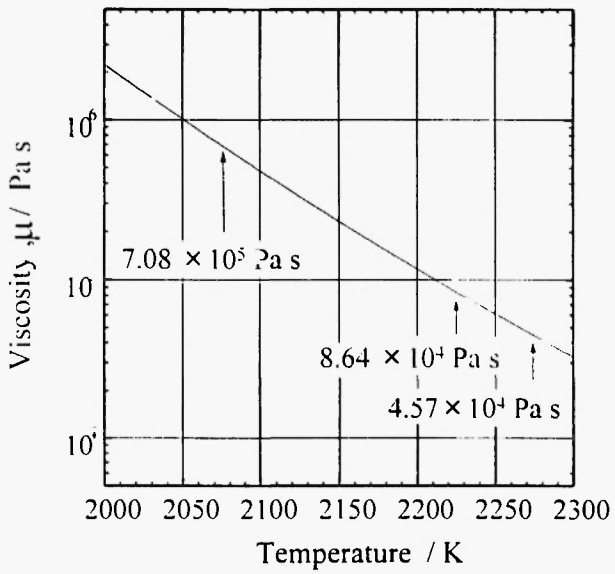

Fig. 14: Relation between the viscosity of SiO_2 (l) and temperature

2073K and 2223K. The lowered viscosity can result in more intensified liquid flow in the vicinity of the SiC tube. In this case, instability can be caused at some locations of the gas film surrounding the SiC tube. The suction of the reaction gas through the tube wall enhances the instability. Then the gas film can be broken and the gas phase forms a bubble, while the direct contact of the liquid phase and the solid phase is established.

Hence we can attribute the difference in the SiO_2-SiC contact between the case of T = 2073~2223K and the case of T – 2273K to the change in the intensity of the liquid flow, due to the change in viscosity of molten SiO_2, in the vicinity of the SiC tube.

The role of the suction of the reaction gas through the tube wall should be mentioned here. In a few preliminary experiments, the authors made experiments without suction to observe the possibility of Si formation at the SiO_2-SiC interface at T = 2273K. The outer look of the SiC tube after these experiments shows that there is no direct contact of SiO_2 with the SiC tube. We can conclude that the suction of the reaction gas through the tube wall is necessary for the direct contact of SiO_2 with the SiC tube.

4.5.5 Rate controlling mechanism

Summarizing the kinetic discussions above, we can illustrate the scheme of the kinetic mechanism of the two step reduction process as seen in Figure 15.

At lower temperature range of T = 2073~2223K (Fig. (15)-(a)), gas phase (gas film) separates the molten

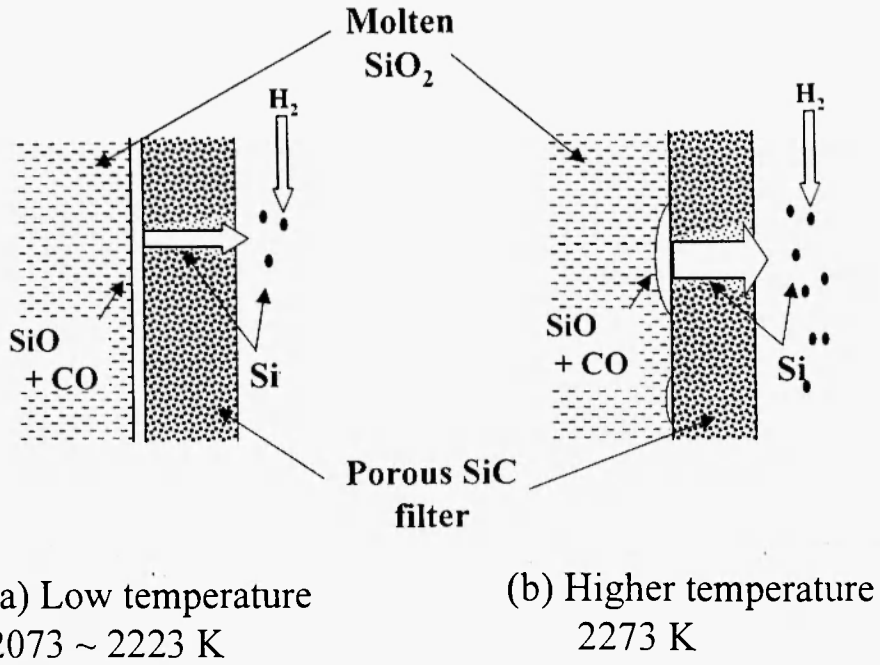

Fig. 15: Schematic mechanism of reduction of SiO_2

SiO_2 phase and the solid SiC phase. The overall reaction rate is controlled by the mass transfer of CO, CO_2 and SiO in the gas phase. Since the rate controlling step is considered to be involved in the 1st stage reduction, i.e. SiO formation reaction step, the gas side mass transfers at SiO_2-gas interface are supposed to be the rate controlling steps.

Thus the apparent independence of the rate of SiO formation on temperature at T = 2073~2223K is interpreted as follows.

The diffusion coefficients of CO, SiO and CO_2 in the gas film increase with the increase in temperature. The increase in temperature also increases the rate constant of the chemical reaction at the gas-SiO_2 interface. The increase in the diffusion coefficients, D, and the rate constant enhances SiO and CO formation rate. The enhanced SiO and CO formation rate tends to increase the thickness of the gas film, δ, to some extent. This increase in the film thickness compensates the increase in the increase in the diffusion coefficient, following the relation that

$$k_i = \frac{D_i}{\delta_i} \qquad [i : \mathrm{SiO, CO, CO_2}]$$

and hence, the mass transfer coefficients, k_{CO}, k_{CO2} and k_{SiO}, do not increase with temperature at T = 2073~2223K.

At the same time, considering the very high temperature (T > 2073K), we can assume that, at T = 2073~2223K where the indirect reaction is predominant, the gas side mass transfer at the gas-SiO_2 interface controls the SiO formation rate dominantly, although we cannot completely avoid the possibility of the interfacial chemical reaction being one of the rate controlling steps. Then we can expect that the increase in temperature does not affect the rate of SiO formation at T = 2073~2223K because of the insensitivity of the mass transfer coefficients to temperature. Thus, the rate constant of SiO formation, $\frac{d\Delta SiO}{dt}$, does not change in the temperature range of T = 2073~2223K (Fig. 12).

At a higher temperature of T = 2073K, (Fig. (15)-(b)), a part of the SiC surface contacts with molten SiO_2. At this part, direct reduction of SiO_2 into SiO takes place.

Here, it should be pointed out that, since the gas phase forms as the results of the reaction, the SiO_2-SiC interface can hardly be stable unless the absence of the reaction. Previously, Bafghi *et al.* //13/ investigated the role of the direct reaction in the case of the smelting reduction of iron oxide in molten slag by graphite. They concluded that the direct reaction between molten slag and graphite was the major reaction of the FeO reduction to Fe and the contribution of the indirect reaction which took place through CO bubble was negligible compared with that of the direct reaction. They further suggested that the direct reaction was possible because of the continuous renewal of the slag-graphite contact area accompanied by a cycling process consisting of the gas phase nucleation, bubble growth and detachment which caused slag flow at the slag-graphite interface. For the present case of SiO_2 reduction into SiO by SiC, we can assume the similar situation for the mechanism of the direct reaction with that suggested by Bafghi *et al.* We thus can explain the results in Figure 12 as follows. According to eq. (47) and the results in Figure 12,

at T = 2073~2223K : $A_{L/G} \gg A_{L/S}$

and at T = 2273K : $A_{L/G} \approx A_{L/S}$, $A_{L/G} k_{OV}^{L/G} \ll A_{L/S} k'_{L/S}$

It should be noted that these relations indicate implicitly that the transfer of oxygen through the mass transfer of CO and CO_2 in the gas phase is much slower than that through the direct reaction.

5. CONCLUSION

In the present study, the authors have proposed a two-stage reduction process for Si production. The fundamental possibilities and the qualitative mechanism of the reactions of the process have been examined by the experiments at 2073~2273K.

The results are summarized as follows.

(1) The formation of Si by the two-stage reduction process is possible at T> 2223K.

(2) The Si formation rate increases vigorously with increasing temperature.

(3) The rate controlling step of the two-stage reduction is involved in the 1st step reduction of SiO_2 into SiO gas.

REFERENCES

1. W. A. Krivsky and R. Schumanm, Jr., *Trans. TMS-AIME*, **221**, 898-904 (1961).
2. M. Nagamori, I. Malinsky, and A. Claveau, *Metall. Trans. B*, **1713**, 503-514 (1986).
3. T. Rosenqvist and J. K. R. Tuset, *Metall. Trans. B*, **1813**, 472-477 (1987).
4. A. Schei and O. Sandberg, *Selected Topics in High Temperature Chemistry*, Forland et al. (eds.), Universitetsforlaget, Oslo, Norway, 1966; p.141-50
5. M. B. Müller, S. E. Olsen, and J. Kr. Tuset, *Scand. J. Metall.*, **1**, 145-155 (1972).
6. A. Schei and K. Larsen, *Electr. Furn. Conf. Proc.*, **39**, 301-309 (1981).
7. K. Suzuki, K. Sakaguchi, T. Nakagiri, and N. Sano, *J. Jpn. Inst. Met.*, **54**, 168-172 (1990).
8. K. Sakaguchi and M. Maeda, *Metall. Trans. B*, **23B**, 423-427 (1992).
9. M. W. Chase, Jr., C. A. Davies, J. R. Downey, Jr., D. J. Frurip, R. A. McDonald, and A. N. Syverud: *JANAF Thermochemical Tables, 3rd ed., J. Phys. Chem. Ref. Data*, 1985, vol. 14, suppl. 1.
10. D. H. Filsinger and D. B. Bourrie, *J. Am. Ceram. Soc.*, **73**, 1726-1732 (1990).
11. K. Yanaba, M. Akasaka, M. Takeuchi, M. Watanabe, T. Narushima, and Y. Iguchi, *Mater. Trans. JIM*, **38**, 990 (1997).
12. The Iron and Steel Institute of Japan, *Handbook of Physico-chemical Properties at High Temperatures*, 140th Committee of Japan Society for Promotion of Science, 1988; p.121.
13. M. S. Bafghi, M. Fukuda, Y. Ito, S. Yamada and M. Sano, *ISIJ International*, **33**, 1125-1130 (1993).